▍**Natural Products**

Sterubin: Enantioresolution and Configurational Stability, Enantiomeric Purity in Nature, and Neuroprotective Activity in Vitro and in Vivo

Julian Hofmann+,[a] Shaimaa Fayez+,[b, c] Matthias Scheiner,[a] Matthias Hoffmann,[a, d] Sabrina Oerter,[e] Antje Appelt-Menzel,[e, f] Pamela Maher,[g] Tangui Maurice,[d] Gerhard Bringmann,*[b] and Michael Decker*[a]

Abstract: Alzheimer's disease (AD) is a neurological disorder with still no preventive or curative treatment. Flavonoids are phytochemicals with potential therapeutic value. Previous studies described the flavanone sterubin isolated from the Californian plant *Eriodictyon californicum* as a potent neuroprotectant in several in vitro assays. Herein, the resolution of synthetic racemic sterubin (**1**) into its two enantiomers, (*R*)-**1** and (*S*)-**1**, is described, which has been performed on a chiral chromatographic phase, and their stereochemical assignment online by HPLC-ECD coupling. (*R*)-**1** and (*S*)-**1** showed comparable neuroprotection in vitro with no significant differences. While the pure stereoisomers were configurationally stable in methanol, fast racemization was observed in the presence of culture medium. We also established the occurrence of extracted sterubin as its pure (*S*)-enantiomer. Moreover, the activity of sterubin (**1**) was investigated for the first time in vivo, in an AD mouse model. Sterubin (**1**) showed a significant positive impact on short- and long-term memory at low dosages.

Introduction

Alzheimer's disease (AD) is an age-associated neurodegenerative disorder and the most common form of dementia (60–80%) among people aged between 65 and 85 years.[1] Pathological hallmarks of the disease include the deposition of amyloid-β (Aβ) containing plaques and tau (τ) containing neurofibrillary tangles.[2] This protein accumulation is accompanied by the loss of neurotrophic factors, ATP depletion, oxidative stress, and neuroinflammation,[3] which lead to neurodegeneration with subsequent cognitive problems and loss of memory.[4]

Over the past few decades, numerous plant-derived natural products have been investigated for their activities against neurodegenerative in vitro hallmarks, including the reduction of oxidative stress, Aβ aggregation, and neuroinflammation.[5] Among these compounds, flavonoids and related polyphenols are powerful antioxidants with potential therapeutic effects.[6] Nevertheless, putative metabolic instability and a potential lack of blood–brain barrier (BBB) penetration are considered as

[a] J. Hofmann,+ M. Scheiner, Dr. M. Hoffmann, Prof. Dr. M. Decker
Pharmaceutical and Medicinal Chemistry
Institute of Pharmacy and Food Chemistry
University of Würzburg
Am Hubland, 97074 Würzburg (Germany)
E-mail: michael.decker@uni-wuerzburg.de

[b] Dr. S. Fayez,+ Prof. Dr. G. Bringmann
Institute of Organic Chemistry
University of Würzburg
Am Hubland, 97074 Würzburg (Germany)
E-mail: bringman@chemie.uni-wuerzburg.de

[c] Dr. S. Fayez+
Department of Pharmacognosy, Faculty of Pharmacy
Ain-Shams University
Organization of African Unity Street 1, 11566 Cairo (Egypt)

[d] Dr. M. Hoffmann, Dr. T. Maurice
MMDN, University of Montpellier
INSERM, EPHE, UMR-S1198
34095 Montpellier (France)

[e] Dr. S. Oerter, Dr. A. Appelt-Menzel
Department for Tissue Engineering and Regenerative Medicine
University Hospital Würzburg
Röntgenring 11, 97070 Würzburg (Germany)

[f] Dr. A. Appelt-Menzel
Translational Center Regenerative Therapies (TLC-RT)
Fraunhofer Institute for Silicate Research ISC
Röntgenring 11, 97070 Würzburg (Germany)

[g] Dr. P. Maher
The Salk Institute for Biological Studies
10010 North Torrey Pines Rd., CA 92037 La Jolla (USA)

[+] These authors contributed equally.

🖳 Supporting information and the ORCID identification number(s) for the author(s) of this article can be found under:
https://doi.org/10.1002/chem.202001264.

Chemistry–A European Journal

Full Paper
doi.org/10.1002/chem.202001264

Chemistry Europe
European Chemical
Societies Publishing

drawbacks regarding "druggability".[7] Recent studies by Schramm et al.[8] and Gunesch et al.[9] have shown a remarkable increase in potency of both flavonoids and flavonolignan derivatives, in vitro and in vivo, by esterification of the hydroxy group at C-7 with phenolic acids. The resulting esters, however, suffer from poor water solubility and high molecular weight.[10]

Recently, Fischer et al.[11] have investigated the extract of *Eriodictyon californicum* (known as yerba santa) from a new pharmacological and medicinal perspective. This plant has long been used for medicinal purposes by native inhabitants of California, where the plant is indigenous.[12] The leaves contain different flavonoids (Figure 1), which are known for their anti-inflammatory and anti-microbial activities against Gram-positive bacteria, and are also used as ingredients in food and pharmaceuticals as bitter-masking agents.[13] Fischer et al. tested extracts of *E. californicum* in a set of age-associated phenotypic screening assays related to AD. They assigned sterubin (7-methoxy-3′,4′,5-trihydroxyflavanone, **1**) as the most active compound in the extract of *E. californicum*, showing a remarkably higher in vitro activity than the co-existing flavonoids eriodictyol (**2**) or homoeriodictyol (**3**).[11] The only very minor structural difference between **1** and **2** demonstrates the "steep" structure–activity relationships of flavonoids. Nothing, however, has so far been reported on the activity of **1** in vivo. Moreover, the chirality of sterubin (**1**), as a result of the stereocenter at C-2, was not taken into consideration, making it unclear which enantiomer was responsible for the activity. Previous re-

ports had shown that flavonoids mainly exist as their respective (*S*)-enantiomers in the plants and that they tend to racemize during the isolation workup procedure.[14] Herein, we report on the synthesis of sterubin (**1**), the chiral resolution of its synthetic racemate, the chiroptical analysis and stereochemical assignment of the (*R*)- and (*S*)-enantiomers, (*R*)-**1** and (*S*)-**1**, online, by HPLC coupled to electronic circular dichroism (ECD), and on the configurational stability of the two stereoisomers. Furthermore, we determined the enantiomeric purity of sterubin in the plant *E. californicum*. Moreover, we describe the in vitro activity of the isolated enantiomers against intracellular oxidative stress using the murine hippocampal neuronal cell line HT22. And, for the first time, we have conducted in vivo investigations on sterubin (**1**) in an AD mouse model with $A\beta_{25-35}$-induced memory impairment[15] and normal mice.

Results and Discussion

Synthesis of sterubin (1)

The synthesis of **1** was performed by analogy to methods for the preparation of similar racemic flavonoids described in the literature.[16] A key step was the condensation of the known[17] acetophenone **7** with the likewise known[18] aldehyde **8** to form the respective chalcone **9** (Scheme 1). Cleavage of the MOM groups and concomitant ring closure was achieved by heating **9** in 10% HCl in MeOH, followed by treatment with sodium acetate to give racemic sterubin (**1**).
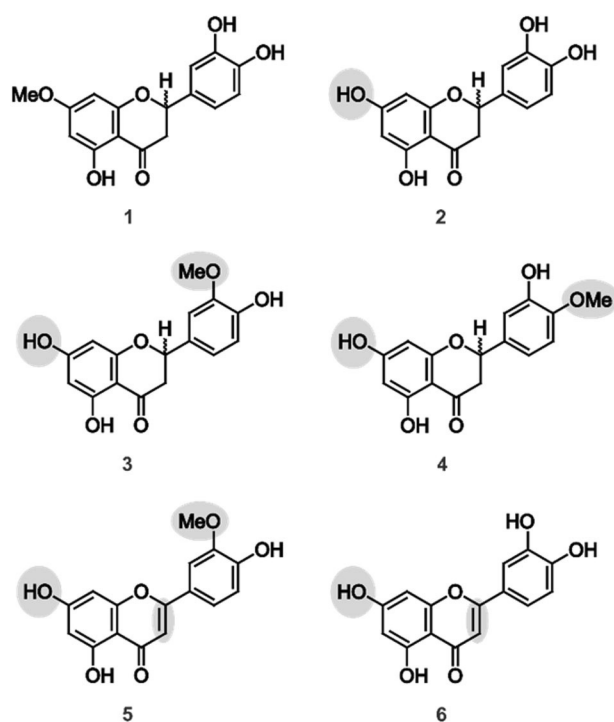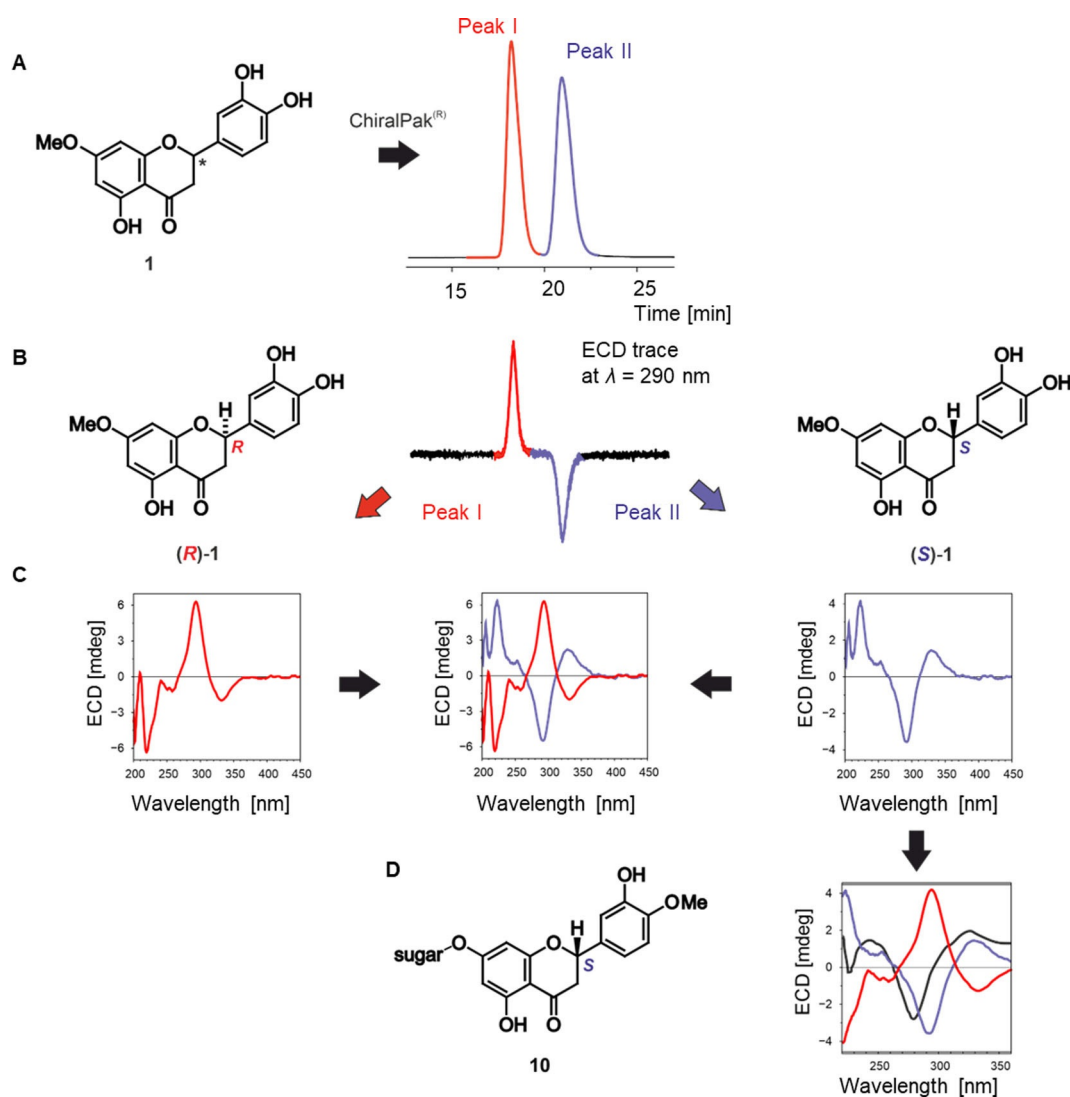

Figure 1. Flavonoids of *Eriodictyon californicum* (yerba santa): sterubin (**1**), eriodictyol (**2**), homoeriodictyol (**3**), hesperetin (**4**), chrysoeriol (**5**), and luteolin (**6**). The structural differences of **2**–**6** as compared to **1** are underlaid in grey.
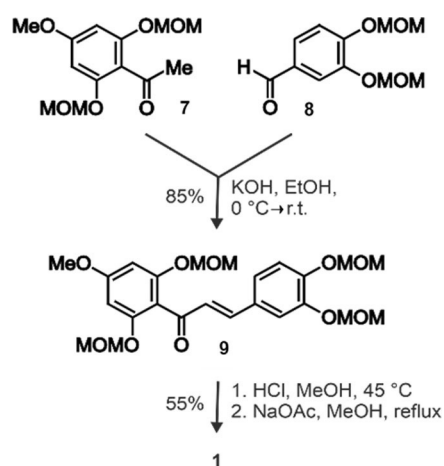
Scheme 1. Key steps in the synthesis of racemic sterubin (**1**). MOM = methoxymethyl.

Resolution of the sterubin enantiomers, (R)-1 and (S)-1

The synthetic racemate of **1** was successfully resolved on a ChiralPak IA® column (10 × 25 mm, 5 µm) using gradient elution with initial condition from 32% B to 60% B in 29 min and a flow rate of 6 mL min⁻¹, where B is 90% acetonitrile in water with 0.05% TFA as a buffer (Figure 2A). Maximum absorption and peak detection was achieved using a PDA detector at $\lambda =$ 290 nm.

Chemistry–A European Journal

Full Paper
doi.org/10.1002/chem.202001264

Chemistry Europe
European Chemical
Societies Publishing

Figure 2. (A) Enantiomeric resolution of racemic sterubin (**1**) on a ChiralPak IA® column; (B) ECD trace (recorded at $\lambda = 290$ nm); (C) online LC-ECD spectra of the two sterubin enantiomers; (D) configurational assignment of the two enantiomers by comparison of their online ECD curves with the offline spectrum reported for the closely related, and configurationally known flavanone glycoside hesperidin (**10**). Sugar = rutinose.
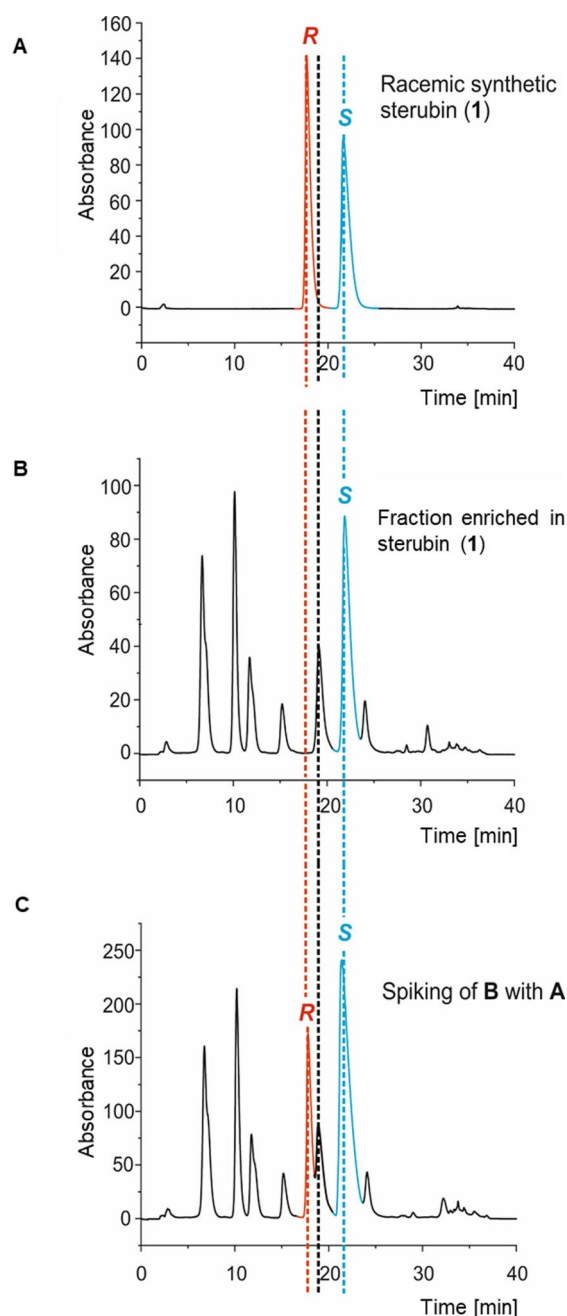
Configurational assignment of the sterubin enantiomers, (R)-1 and (S)-1, by HPLC-ECD coupling

The absolute configuration of the two resolved peaks was assigned online, by HPLC-ECD coupling.[19] By measurement at a single wavelength, 290 nm, the chiroptically opposite behavior of the two peaks was clearly seen (Figure 2B), further supporting the assumption that the compounds were indeed enantiomers. This was corroborated by the full online ECD spectra showing a first, negative couplet at 330 nm (Peak **I**) and a second, positive one at 290 nm (Peak **II**) for the fast enantiomer and an opposite curve for the slower peak (Figure 2C). The assignment of the rapidly eluting peak as corresponding to the R-enantiomer of sterubin, (R)-**1**, and the slower one as its (S)-configured isomer, (S)-**1**, was achieved by comparison of the ECD spectra of the two enantiomers with that of the known, closely related, S-configured flavanone glycoside hesperidin (**10**) (Figure 2D).[20] The ECD curve of the second peak

(Peak **II**) showed a good match with the spectrum of **10**, hence the slower enantiomer was S-configured. For the first peak, by contrast (Peak **I**), virtually opposite spectra were detected, so the faster eluting enantiomer was (R)-**1**.

Assignment of the absolute configuration and enantiomeric purity of sterubin (1) in *Eriodictyon californicum*

Most naturally occurring flavonoids have so far been isolated as the respective (S)-enantiomers.[14] To investigate the absolute configuration and the enantiomeric purity of sterubin (**1**) in *E. californicum*, dried leaves of the plant were extracted by mild maceration in ethyl acetate assisted by ultrasonication for 30 min at room temperature. Sterubin (**1**) and related flavanones were enriched by precipitation from the ethyl acetate crude extract after addition of *n*-hexane. The resulting precipitate was filtered, dissolved in methanol, and injected on a ChiralPak IA® column (Figure 3B). Spiking experiments with the

Chemistry–A European Journal

Full Paper
doi.org/10.1002/chem.202001264

Chemistry Europe
European Chemical
Societies Publishing

Figure 3. Chromatograms on a ChiralPak IA® column: (A) synthetic racemic sterubin (**1**); (B) the extract enriched with **1**; (C) coelution of **1** with the extract enriched with racemic **1** showing an increase in the peak intensity of the (S)-enantiomer and evidencing that in *E. californicum*, sterubin (**1**) is produced in an enantiopure S-form, (S)-**1**.

synthetic racemate of **1** (Figure 3 A) revealed an increase in the peak intensity of the S-enantiomer (Figure 3 C), showing that the plant contained sterubin (**1**) in an enantiomerically pure form, as its (S)-enantiomer, (S)-**1**. No racemization had occurred during the extraction procedure described, while extraction under reflux conditions as described in the literature[13a] obviously can lead to racemization.

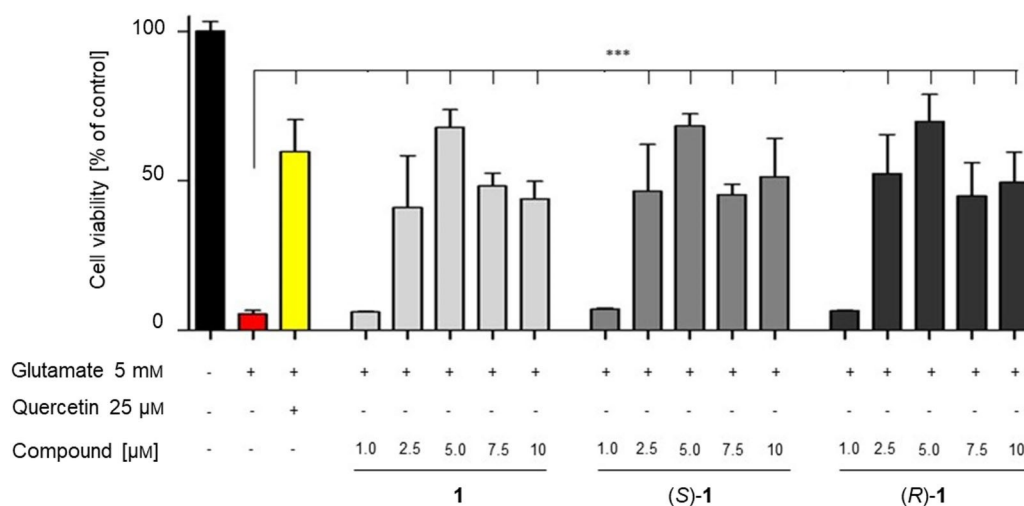## Configurational stability of the sterubin enantiomers (R)-1 and (S)-1

For an investigation of the configurational stability of sterubin, its pure enantiomers, (R)-**1** and (S)-**1**, were kept dissolved in methanol at room temperature and the solution was monitored for the formation of the other respective enantiomer by HPLC on a ChiralPak IA® column after 2, 20, and 44 h. Under the applied conditions, the two enantiomers proved to be configurationally fully stable over 2 d and no racemization was observed as seen in Figure 4.
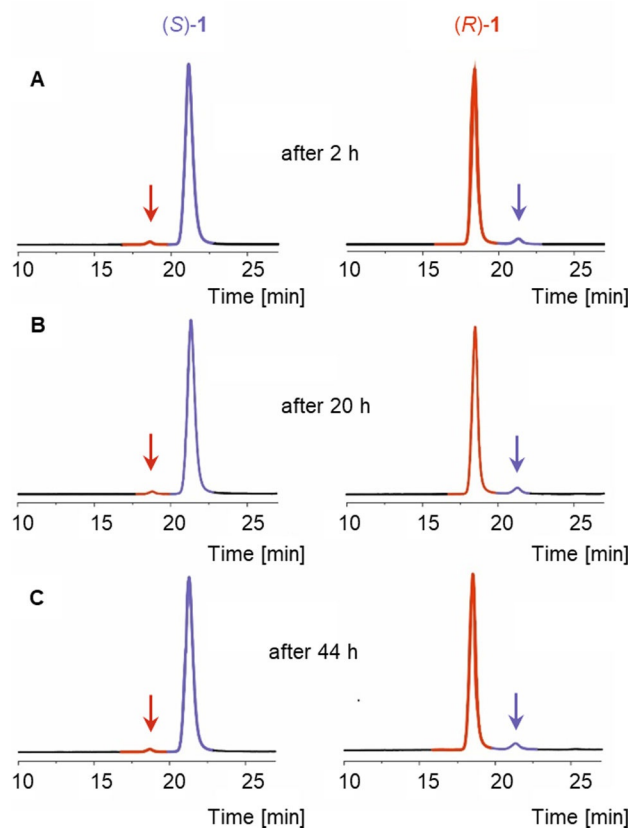
Figure 4. Stability studies on the (R)- and (S)-enantiomers of sterubin, (R)-**1** and (S)-**1**, in methanol: (A) after 2 h; (B) after 20 h; (C) after 44 h on a Chiral-Pak IA® column. The enantiomers were configurationally stable over the entire time. The arrows indicate the expected sites of the respective minor enantiomer.

Oxytosis assay

HT22 cells are a murine hippocampal nerve cell line. They are sensitive to oxidative glutamate toxicity (oxytosis) due to a lack of ionotropic glutamate receptors.[9–10, 21] Addition of high concentrations of extracellular glutamate inhibits the transport of cystine, the oxidized form of cysteine, via the cystine/glutamate antiporter, which results in glutathione (GSH) depletion. The consecutive accumulation of ROS and calcium leads to intracellular oxidative stress followed by cell death.[22] As GSH depletion is similarly observed during aging of the brain and is even accelerated in AD, the oxytosis assay gives information

Chemistry–A European Journal

Full Paper
doi.org/10.1002/chem.202001264

**Chemistry Europe**
European Chemical
Societies Publishing

Figure 5. Oxytosis assay: Treatment of HT22 cells with 5 mM glutamate (red) induced cytotoxicity. Quercetin (yellow) served as a positive control, **1**, (*S*)-**1**, and (*R*)-**1** all showed the same neuroprotective efficacy. Data are presented as means ± SEM of three independent experiments and results refer to untreated control cells (black). Statistical analysis was performed using One-Way ANOVA followed by Dunnett's multiple comparison posttest using GraphPad Prism 5 referring to cells treated with 5 mM glutamate. Level of significance: *** $p < 0.001$.

about the neuroprotective properties of **1** against oxidative stress in cells.[23] Flavonoids generally have only moderate antioxidant properties[24] and, as reported by Fischer et al., sterubin (**1**) is one of the more potent flavonoids against oxidative stress and neuroinflammation in vitro.[11] The pure enantiomers of sterubin, (*R*)-**1** and (*S*)-**1**, as well as the synthetic racemic mixture, were investigated in the oxytosis assay to identify possible differences in activity between the stereoisomers. The flavonol quercetin at a high concentration (25 μM) served as a positive control (Figure 5). Unexpectedly, no difference in activity was observed between the racemic mixture and any of the pure enantiomers. All of them provided significant neuroprotection at concentrations from 2.5 μM to 10 μM, which even exceeded that of the positive control quercetin at a concentration of 5 μM. The lack of a difference in bioactivity between the pure enantiomers (and between them and the racemic mixture) raised the question whether the pure enantiomers might possibly undergo racemization upon contact with cells or even upon exposure to the culture medium, in contrast to their proven configurational stability in methanol (see above).
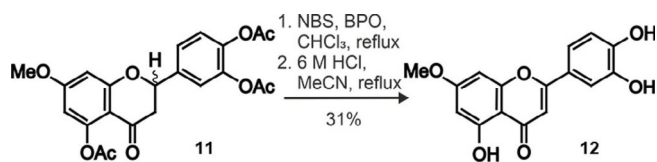
Cellular uptake and racemization

Vrba et al.[25] and Gunesch et al.[9] observed the formation of dehydrogenated products of esters combining the flavonoid taxifolin and polyphenolic acids in RAW264.7 macrophages or BV-2 microglia. In the case of sterubin (**1**), this would cause a loss of the stereogenic center at C-2, which would explain why the same activities were found for **1**, (*S*)-**1**, and (*R*)-**1**. Another explanation could be racemization in the cell culture medium. Therefore, we investigated cellular uptake experiments in microglial BV-2 cells and performed stability measurements in cell culture medium. BV-2 cells were treated with 50 μM of the respective compounds and incubated for 2 h or 4 h or lysed immediately, respectively. Lysates were analyzed by HPLC on a

chiral-phase column and LC-UV. Reference chromatograms with sterubin (**1**) and dehydrosterubin (**12**) were recorded beforehand. As seen in Figure 6, sterubin (**1**) is chemically stable in the BV-2 cells. While no conversion of sterubin (**1**) to dehydrosterubin (**12**) was found (Scheme 2), HPLC on a chiral stationary phase revealed rapid racemization in the cell culture medium even without the presence of cells (cf. Supporting Information).
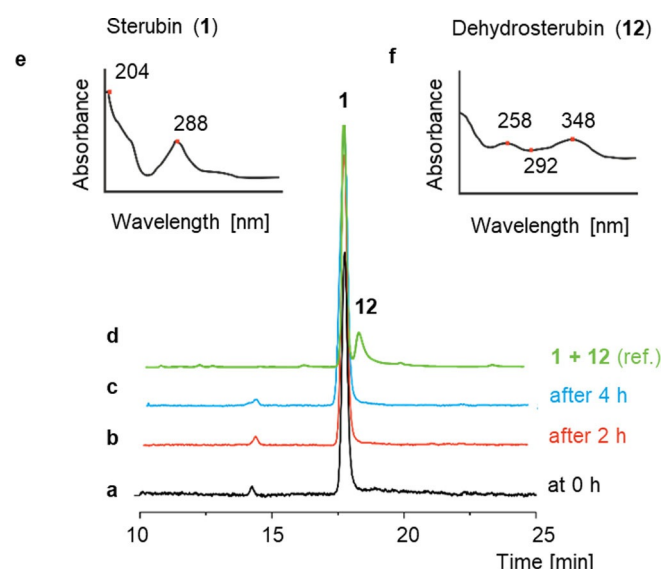
Figure 6. The chemical stability of (*R*)-**1** in BV-2 cells assigned by HPLC/UV: (a) at 0 h (black), (b) after 2 h (red), and (c) after 4 h (blue) of incubation, (d) reference chromatogram of **1** and dehydrosterubin (**12**) (green); (e) UV spectra of **1**; (f) UV spectra of **12**. (*R*)-**1** was chemically stable over the whole time.

Chemistry–A European Journal

Full Paper
doi.org/10.1002/chem.202001264

Chemistry Europe
European Chemical
Societies Publishing

Scheme 2. Final steps in the synthesis of dehydrosterubin (**12**).

Synthesis of dehydrosterubin

Dehydrosterubin (**12**), also named hydroxygenkwanin, as a reference compound was synthesized by analogy to a procedure described by Aft.[26] For this purpose, the triacetate **11**[16] of sterubin (**1**) was dehydrogenated with *N*-bromosuccinimide (NBS) in the presence of catalytic amounts of benzoyl peroxide (BPO) to give the respective dehydro compound. Deprotection was accomplished in 6 M $HCl_{(aq.)}$ in acetonitrile, resulting in dehydrosterubin (**12**).

Neuroprotection in vivo

Recently, a number of polyphenols, including synthetic compounds as well as natural products, have been identified as potent neuroprotective agents in vitro.[9, 11, 25] Surprisingly, sterubin (**1**) showed a higher activity against oxidative stress and neuroinflammation than several other flavonoids.[11] To determine if sterubin (**1**) also has neuroprotective effects in vivo, experiments were performed using a mouse model of AD described previously.[15, 27] Beforehand, in vitro cytotoxicity experiments with human induced pluripotent stem cell derived blood brain barrier endothelial cells were performed (cf. Supporting Information) to exclude toxicity. The results demonstrate, that **1** did not have any major toxic effects. For the in vivo studies described in this work, AD-like neurotoxicity and memory impairments were induced by intracerebroventricular (ICV) injection of the amyloid β (Aβ) fragment $Aβ_{25–35}$ (9 nmol) on the first day of the study. Control mice received distilled water (V1) ICV. Racemic sterubin (**1**) was dissolved in a mixture of 60% DMSO and 40% saline (0.9% NaCl in milliQ water) and the solutions were injected intraperitoneally (IP) once per day (o.d.) for the following 7 d at doses between 0.3 and 3 mg kg⁻¹ of **1**. Injections of vehicle (60% DMSO+40% saline, V2) were used for the two control groups. Sterubin did not affect the mouse body weight gain during the period of treatment (cf. Supporting Information). Short-term spatial memory was evaluated in the Y-maze test (YMT) on day 8 and long-term memory was evaluated on days 9 (training) and 10 (measurement of step-through latency) in the step-through passive-avoidance assay (STPA). On day 11, the mice were sacrificed, and the brains were frozen at −80°C. Sterubin (**1**) significantly improved the $Aβ_{25–35}$-induced alternation deficit in the YMT at doses greater than 1 mg kg⁻¹ (Figure 7 A), further substantiating the neuroprotective effects observed in vitro.[11] In agreement with the results obtained in the YMT (Figure 7 A), the $Aβ_{25–35}$-induced deficit in long-term memory was also compensated at a dose of sterubin (**1**) of 1 mg kg⁻¹ or higher (Figure 7 B). Sterubin (**1**) exceeded the activity of previously studied polyphenols such as silibinin and taxifolin used in the same mouse model of AD with respect to the dose needed to compensate for the $Aβ_{25–35}$ induced effects.[9, 28]
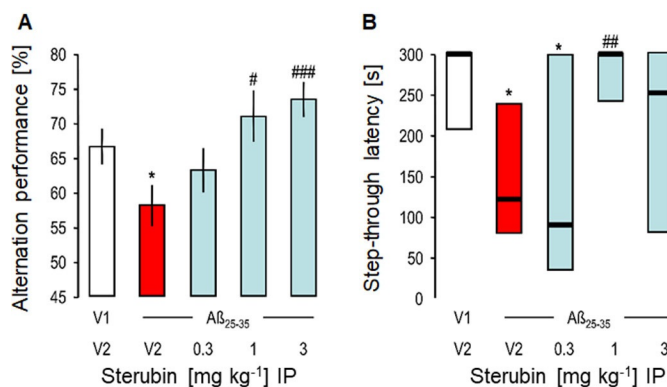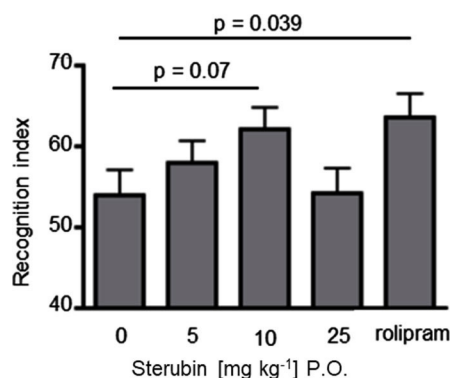

Figure 7. Effect of sterubin (**1**), administered IP, on $Aβ_{25–35}$-induced learning impairments in mice: (A) spontaneous alternation performance in YMT and (B) step-through latency in the STPA. Animals obtained distilled water (V1) or $Aβ_{25–35}$ (9 nmol ICV) on day 1 and received sterubin (0.3–3 mg kg⁻¹ IP), or DMSO 60% in saline (V2), o.d. between day 1 and 7. They were examined in the YMT on day 8 and passive avoidance training was performed on day 9, with retention being tested after 24 h. Data show mean ± SEM in (A) and median and interquartile range in (B). $n = 12$–18 per groups. ANOVA: $F_{(4,57)} = 3.85$, $p < 0.01$ in (A). Kruskal-Wallis ANOVA: $H = 11.6$, $p < 0.05$ in (B). * $p < 0.05$ vs. (V+V)-treated group; # $p < 0.05$, ## $p < 0.01$, ### $p < 0.001$ vs. (V+$Aβ_{25–35}$)-treated group; Dunnett's test in (A), Dunn's test in (B).

Effects on memory in normal mice

We also asked if sterubin could improve memory in normal mice as was previously shown for the flavonol fisetin using the object recognition test.[29] In this test, mice are presented with two identical objects during the training period, which they explore for a fixed time period. To test for memory, mice are presented one day later with two different objects, one of which was presented previously during the training and is thus familiar to the mice, and the other that is novel. The better a mouse remembers the familiar object, the more time it will spend exploring the novel object. To test the effects of sterubin in this memory task, it was administered orally to the mice before the start of the training period. Rolipram, a phosphodiesterase inhibitor that potentiates memory in this assay,[30] requires intraperitoneal injection and was used as a positive control. As shown in Figure 8, three doses of sterubin were tested in the object recognition task and 10 mg kg⁻¹ showed a strong but not quite significant effect.

Conclusions

By HPLC on a chiral phase column, resolution of synthetically prepared racemic sterubin (**1**) into its pure enantiomers, (*R*)-**1** and (*S*)-**1**, was achieved for the first time. Although in methanol configurational stability was observed, racemization took place in the cell culture medium. These findings explain why no difference in the neuroprotective activity in HT22 cells was found between racemic sterubin (**1**) and its pure enantiomers.

Chemistry–A European Journal

Full Paper
doi.org/10.1002/chem.202001264

Chemistry Europe
European Chemical
Societies Publishing

Figure 8. Effect of sterubin (**1**) on memory in normal mice. Sterubin moderately enhances long-term memory in mice. The effect of different oral doses of sterubin on object recognition over a 10 min test period. Rolipram, injected intraperitoneally at 0.1 mg kg⁻¹, served as a positive control. Data represent the mean ± SEM of 11 mice/treatment group. Data were analyzed by one-way ANOVA followed by post-hoc comparisons with Fisher's test.

Importantly, in vivo experiments revealed the high potency of sterubin as a neuroprotective agent against $A\beta_{25-35}$-induced AD-like memory loss in mice. The effects were observed in both short-term and long-term memory assays. Lesser effects on cognition were seen in normal mice suggesting that the cognitive improvements were not simply symptomatic in nature. It can be concluded that sterubin (**1**) exhibits strong neuroprotective properties during the 7-day treatment, leading to improved memory in the behavioral tests after the treatment was stopped. Hence, these findings strongly support that sterubin (**1**) holds significant potential as a disease-modifying neuroprotectant in AD.

Experimental Section

General: All reagents were bought from Sigma Aldrich, Munich, Germany, unless otherwise noted, and were used without further purification. Thin-layer chromatography was performed using Merck Silica Gel 60 F$_{254}$ plates. For column chromatography, Silica Gel 60 (particle size 0.040–0.063 mm) (Sigma Aldrich, Munich, Germany) was used. Nuclear magnetic resonance (NMR) spectra were recorded with a Bruker AV-400 NMR instrument (Bruker, Karlsruhe, Germany) in CDCl$_3$ or [D$_6$]DMSO. Chemical shifts are expressed in ppm relative to CDCl$_3$ (7.26 ppm for ^{1}H and 77.16 ppm for ^{13}C) or [D$_6$]DMSO (2.50 ppm for ^{1}H and 39.52 ppm for ^{13}C). The purity of the synthetic products was determined by HPLC (Shimadzu, Duisburg, Germany), containing a DGU-20A3R degassing unit, an LC-20AB liquid chromatograph, and an SPD-20A UV/Vis detector. UV detection was done at 254 nm. Mass spectra were obtained by an LCMS-2020 device (Shimadzu, Duisburg, Germany). As a stationary phase, a Synergi 4U fusion-RP column (150 mm x 4.6 mm) was used, and, as a mobile phase, a gradient of methanol/water with 0.1% formic acid. Parameters: A=water, B=methanol, V(B)/[(V(A)+ V(B)]=from 5% to 90% over 10 min, V(B)/[(V(A)+V(B)]=90% for 5 min, V(B)/[(V(A)+V(B)]=from 90% to 5% over 3 min. The method was performed with a flow rate of 1.0 mL min⁻¹. Compounds were used for biological evaluation only if the purity was 95% or higher.

For the preparation of acetophenone **7** and aldehyde **8**, see the Supporting Information.

Chalcone 9: A mixture of acetophenone **7** (650 mg, 2.16 mmol) in EtOH (10 mL) and a saturated solution of KOH in EtOH (15 mL) was stirred at 4°C for 15 min. A solution of **8** (490 mg, 2.16 mmol) in EtOH (5 mL) was added dropwise and the mixture was allowed to stir overnight (16 h) at room temperature. The reaction was quenched with water and extracted with ethyl acetate. The combined organic layers were dried over Na$_2$SO$_4$ and the solvent was removed under reduced pressure. The crude product was purified by silica gel chromatography using a mixture of cyclohexane and ethyl acetate (3/1). The product was obtained as a yellow solid in 85% yield (1.11 g). The analytical data were consistent with those reported in the literature.[31] ^{1}H NMR (400 MHz, CDCl$_3$): δ 7.35 (s, 1H, Ar-H), 7.26 (d, ^2J=16.0 Hz, 1H, HC=CH), 7.13 (s, 2H, Ar-H), 6.86 (d, ^2J=16.0 Hz, 1H, HC=C*H*), 6.43 (s, 2H, Ar-H), 5.25 (s, 2H, C*H$_2$*OCH$_3$), 5.22 (s, 2H, C*H$_2$*OCH$_3$), 5.11 (s, 4H, C*H$_2$*OCH$_3$), 3.82 (s, 3H, OC*H$_3$*), 3.51 (s, 3H, CH$_2$OC*H$_3$*), 3.50 (s, 3H, CH$_2$OC*H$_3$*), 3.39 ppm (s, 6H, CH$_2$OC*H$_3$*); ^{13}C NMR (100 MHz, CDCl$_3$): δ 194.4 (C$_q$, C=O), 162.1 (C$_q$, Ar-C), 156.0 (2x C$_q$, Ar-C), 149.4 (C$_q$, Ar-C), 147.5 (C$_q$, Ar-C), 144.7 (+, HC=CH), 129.4 (C$_q$, Ar-C), 128.1 (+, HC=CH), 123.8 (+, Ar-C), 116.3 (+, Ar-C), 116.0 (+, Ar-C), 113.8 (C$_q$, Ar-C), 95.6 (−, CH$_2$OCH$_3$), 95.2 (−, CH$_2$OCH$_3$), 95.1 (2×+, Ar-C), 94.6 (2x, −, CH$_2$OCH$_3$), 56.5 (+, CH$_2$OCH$_3$), 56.4 (+, CH$_2$OCH$_3$), 56.3 (2©+, CH$_2$OCH$_3$), 55.6 ppm (+, OCH$_3$); ESI-MS: m/z calcd for C$_{24}$H$_{30}$O$_{10}$+H$^+$: 479.19; found 479.2.

Sterubin (1): A solution of chalcone **9** (1.10 g, 2.32 mmol) in 10% methanolic HCl was stirred for 30 min at 50°C. NaOAc (3.80 g, 46.4 mmol) was added and the mixture was heated to reflux for 3 h, cooled, then water was added and the mixture was extracted with ethyl acetate. The combined organic layers were dried over Na$_2$SO$_4$ and the solvent was removed under reduced pressure. The crude product was purified by silica gel column chromatography using a mixture of dichloromethane and methanol (40/1) as the eluent. The product was obtained as a white solid in 55% yield (391 mg). The analytical data were consistent with those reported in the literature.[13a] ^{1}H NMR (400 MHz, [D$_6$]DMSO): δ 12.11 (s, 1H, O*H*), 9.03 (m, 2H, O*H*), 6.91–6.86 (m, 1H, Ar-H), 6.78–6.71 (m, 2H, Ar-H), 6.10 6.06 (m, 2H, Ar-H), 5.42 (dd, ^3J=12.6, 3.0 Hz, 1H), 3.79 (s, 3H, OC*H$_3$*), 3.24 (dd, ^2J=17.2, ^3J=12.6 Hz, 1H), 2.72 (dd, ^2J=17.2, ^3J=3.1 Hz, 1H); ^{13}C NMR (100 MHz, [D$_6$]DMSO): δ 196.9 (C$_q$, C=O), 167.4 (C$_q$, Ar-C), 163.1 (C$_q$, Ar-C), 162.8 (C$_q$, Ar-C), 145.7 (C$_q$, Ar-C), 145.1 (C$_q$, Ar-C), 129.2 (C$_q$, Ar-C), 117.9 (+, Ar-C), 115.3 (+, Ar-C), 114.3 (+, Ar-C), 102.6 (C$_q$, Ar-C), 94.5 (+, Ar-C), 93.7 (+, Ar-C), 78.6 (+, Ar-C), 55.8 (+, C*H$_3$* OC*H$_3$*), 42.1 (−, CH$_2$). ESI-MS: m/z calcd for C$_{16}$H$_{15}$O$_6$+H$^+$: 303.09; found 303.15.

For the preparation of **11**, see the Supporting Information.

Tri-O-acetyldehydrosterubin: To a solution of tri-O-acetylsterubin (**11**) (160 mg, 0.374 mmol) and NBS (67 mg, 0.374 mmol) in chloroform (5 mL) benzoyl peroxide (6 mg, 26 μmol) was added and the reaction mixture was heated to reflux for 2 h. Further chloroform was added, and the mixture was washed with water and brine. The organic layer was dried over Na$_2$SO$_4$ and the solvent was removed under reduced pressure. The crude product was purified by silica gel chromatography using an eluent of cyclohexane and ethyl acetate (2:1 → pure ethyl acetate) and the product was obtained as a white solid in 63% yield (100 mg). ^{1}H NMR: (400 MHz, CDCl$_3$): δ 7.73 (dd, ^3J=8.5, ^4J=2.2 Hz, 1H, Ar-H), 7.70 (d, ^4J=2.1 Hz, 1H, Ar-H), 7.35 (d, ^3J=8.5 Hz, 1H, Ar-H), 6.87 (d, ^4J=2.5 Hz, 1H, Ar-H), 6.62 (d, ^4J=2.4 Hz, 1H, Ar-H), 6.55 (s, 1H, C=CH), 3.92 (s, 3H, OC*H$_3$*), 2.44 (s, 3H, C*H$_3$*COO), 2.35 (s, 3H, C*H$_3$*COO), 2.33 (s, 3H, C*H$_3$*COO); ^{13}C NMR (100 MHz, CDCl$_3$): δ 176.3 (C$_q$, C=O), 169.7 (C$_q$, CH$_3$*C*OO), 168.1 (C$_q$, CH$_3$*C*OO), 167.9 (C$_q$, CH$_3$*C*OO), 163.7 (C$_q$, Ar-C), 160.3 (C$_q$, C=CH), 158.9 (C$_q$, Ar-C), 150.7 (C$_q$, Ar-C), 144.7 (C$_q$, Ar-C), 142.7 (C$_q$, Ar-C), 130.2 (C$_q$, Ar-C), 124.5 (+, Ar-C), 124.3 (+, Ar-C),

Chemistry–A European Journal

Full Paper
doi.org/10.1002/chem.202001264

**Chemistry
Europe**
European Chemical
Societies Publishing

121.6 ($+$, Ar-C), 111.3 (C_q, Ar-C), 109.0 ($+$, C=CH), 108.6 ($+$, Ar-C), 99.2 ($+$, Ar-C), 56.1 ($+$, OCH_3), 21.2 (CH_3COO), 20.8 (CH_3COO), 20.7 (CH_3COO); ESI-MS: m/z calcd for $C_{22}H_{18}O_9 + H^+$: 427.10; found 427.20.

Dehydrosterubin (12): A solution of tri-O-acetyldehydrosterubin (97 mg, 0.227 mmol) in acetonitrile (3 mL) and conc. aqueous HCl (3 mL) was heated to reflux for 1.5 h. Yellow precipitant was formed, which was filtered off, washed with water, and dried under vacuum. The product was obtained as a yellow solid in 50 % yield (34 mg). ^{1}H NMR (400 MHz, [D_6]DMSO): δ 12.97 (s, 1H, OH), 9.96 (s, 1H, OH), 9.37 (s, 1H, OH), 7.44 (m, 2H, Ar-H), 6.90 (d, $^3J = 8.1$ Hz, 1H, Ar-H), 6.72 (s, 1H, C=CH), 6.71 (d, $^4J = 2.5$ Hz, 1H, Ar-H), 6.37 (d, $^4J = 2.2$ Hz, 1H, Ar-H), 3.87 (s, 3H, OCH_3); ^{13}C NMR (100 MHz, [D_6]DMSO): δ 181.7 (C_q, C=O), 165.0 (C_q, Ar-C), 164.2 (C_q, Ar-C), 161.1 (C_q, C=CH), 157.1 (C_q, Ar-C), 149.8 (C_q, Ar-C), 145.7 (C_q, Ar-C), 121.3 (C_q, Ar-C), 119.0 ($+$, Ar-C), 115.9 ($+$, Ar-C), 113.5 ($+$, Ar-C), 104.6 (C_q, Ar-C), 103.0 ($+$, C=CH), 97.9 ($+$, Ar-C), 92.5 ($+$, Ar-C), 56.0 ($+$, OCH_3); ESI-MS: m/z calcd for $C_{16}H_{12}O_6 + H^+$: 301.07; found 301.15.

Plant material: Leaves of *Eriodictyon californicum* Hook. & Arn. (Boraginaceae) were collected by Ms. Kyra Bobine in May, 2019.

Plant extraction: Dried leaves of *E. californicum* (18.6 g) were soaked in ethyl acetate (3×100 mL), ultrasonicated for 30 min, then shaken overnight ($\approx$16 h) at room temperature. The crude extract was filtered, and the filtrate was concentrated in vacuo. The obtained residue (2.0 g) was re-dissolved in 90 % aqueous methanol. By addition of *n*-hexane, chlorophyll and non-polar residues were removed and sterubin (**1**) and related flavones were precipitated. After filtration, the precipitate (0.6 g) was dissolved in methanol and directly subjected to HPLC on a ChiralPak-IA column.

Chiral resolution of racemic sterubin: An HPLC-UV guided resolution of the enantiomers of **1** was performed on a Jasco system equipped with a DG-2080 degassing unit, a PU-1580 ternary pump, an MD-2010 plus multiwavelength detector, and an AS-2055 auto-sampler. Separation of the enantiomers was done on a ChiralPak IA® (10×25 mm, 5 μm, Daicel Chemical Industries) column using a gradient system with initial conditions 32 % B (B: 90 % MeCN in water + 0.05 % TFA) to 60 % B in 29 min. The (R)- and (S)-enantiomers of sterubin, (R)-**1** and (S)-**1**, had retention times of 17.8 min and 20.2 min, respectively.

Online LC-ECD analysis of the sterubin enantiomers: ECD spectroscopic analysis was performed using a Jasco J-715 spectropolarimeter. Measurements were done at room temperature and the spectra were processed using the SpecDis software.[32]

Oxytosis assay: HT22 cells were grown in Dulbecco's Modified Eagle Medium (DMEM, Sigma Aldrich, Munich, Germany) supplemented with 10 % (v/v) fetal calf serum (FCS) and 1 % (v/v) penicillin-streptomycin. 5×10^3 HT22 cells per well were seeded into sterile 96-well plates and incubated overnight ($\approx$16 h). Aqueous glutamate solution (5 mm) (monosodium-L-glutamate, Sigma Aldrich, Munich, Germany) together with 2.5, 5.0, 7.5, or 10 μM of the respective compound was added to the cells and incubated for 24 h. Quercetin (25 μM) (Sigma Aldrich, Munich, Germany) together with glutamate (5 mm) served as a positive control. After 24 h incubation cell viability was determined using a colorimetric 3-(4,5-dimethylthiazol-2-yl)-2,5-diphenyltetrazolium bromide (MTT, Sigma Aldrich, Munich, Germany) assay. MTT solution (5 mg mL^{-1} in PBS) was diluted 1:10 with medium and added to the wells after removal of the old medium. Cells were incubated for 3 h and then lysis buffer (10 % SDS) was added. The next day, absorbance at 560 nm was determined with a multiwell plate photometer (Tecan, Spectra-

Max 250). Results are presented as percentage of untreated control cells. All data are expressed as means ± SEM of three independent experiments. Analysis was accomplished using GraphPad Prism 5 Software applying Oneway ANOVA followed by Dunnett's multiple comparison posttest. Levels of significance: * $p < 0.05$; ** $p < 0.01$; *** $p < 0.001$.

Cellular uptake and racemization experiments: 2×10^6 BV2 cells were grown in sterile 100 mm dishes overnight and 4 mL 50 μM (S)-**1** or (R)-**1** diluted in cell culture medium were added. Cells were incubated for the indicated time periods, after which the supernatant was removed, and cells were washed twice with PBS. Further PBS (1 mL) was added, cells were scraped and transferred to Eppendorf tubes. The samples were centrifuged and resuspended in 200 μL of MeOH. The cells were frozen in liquid nitrogen and thawed at 37 °C (10 times). Cell debris was pelleted by centrifugation and the supernatant was collected for HPLC analysis.

Neuroprotection studies in vivo: The in vivo behavioral experiments were performed as established and published previously.[15,33] Neurotoxicity was induced by ICV injection of oligomerized Aβ$_{25-35}$ peptide, and sterubin (**1**) was evaluated for its neuroprotective properties. Sterubin was dissolved in 60 % DMSO and 40 % saline (0.9 % NaCl in milliQ water) and was injected once per day IP on days 1–7 to give doses of 0.3, 1, and 3 mg kg^{-1}. The oligomerized Aβ$_{25-35}$ peptide was injected ICV on day 1 of the study. The behavior of the mice was evaluated on day 8 (YMT) and days 9 and 10 (STPA). On day 11, the mice were sacrificed, and the brains were collected. Samples were frozen at −80 °C for further biochemical analysis.

Animals: Male Swiss mice 6 weeks old, body weight 30–40 g, obtained from JANVIER (Saint Berthevin, France) were housed in the animal facility of the University of Montpellier (CECEMA, Office of Veterinary Services agreement #B-34-172-23) with access to food and water *ad libitum* (except during behavioral tests). The humidity and temperature were controlled, and the mice were kept at a 12 h light/12 h dark cycle (lights off at 7:00 p.m.). All animal procedures were conducted in strict adherence to the European Union directives of September 22nd, 2010 (2010/63/UE) and to the ARRIVE guidelines. The project was authorized by the French National Ethics Committee (APAFIS #1485-15034). Animals were assigned to different treatment groups randomly.

Preparation of sterubin injections: Sterubin (**1**) was dissolved in 100 % DMSO at a concentration of 6 mg mL^{-1} to give a stock solution, which was diluted with saline (0.9 % NaCl in milliQ water) and DMSO to the final test concentration and a final percentage of 60 % DMSO. 60 % DMSO in saline served as the vehicle (V2). After compound injections, the behavior of the mice in their home cage was checked visually. Weight was examined once per day. As demonstrated in Figure S1, a tendency was observed that weight gain was facilitated with an increasing dose of **1**. Nevertheless, the difference in weight gain remained insignificant compared to Aβ+V2 treated mice in Dunnett's multiple comparison test.

Amyloid peptide preparation and ICV injection: All experiments followed previously described protocols.[15,25,32] The Aβ$_{25-35}$ peptide was prepared according to Maurice et al.[15] Mice were anesthetized with 2.5 % isoflurane. Then, oligomerized Aβ$_{25-35}$ peptide (9 nmol in 3 μL/mouse) was injected ICV. Bidistilled water was used as a vehicle (V1).

Spontaneous alternation performance in a Y-maze: On day 8 of the study, the spatial working memory of all mice was evaluated in the Y-maze.[15,25,32] The Y-maze is made from grey polyvinylchloride and has three identical arms (length 40 cm, height 13 cm, bottom width 3 cm, top width 10 cm (walls converge at an equal angle).

For evaluation of memory, every mouse was placed into one arm and was allowed to explore the maze for 8 min. All entries into an arm (including the return into the same arm) were counted and the number of alternations (mouse entered all three arms consecutively) was calculated as percentage of total number of arm entries [alternations/ (arm entries−2)×100].

Step-through passive avoidance test: STPA was performed on day 9 and day 10 in a two-compartment box [(width 10 cm, total length 20 cm (10 cm per compartment), height 20 cm] consisting of polyvinylchloride. One of the compartments was white and illuminated with a bulb (60 W, 40 cm above the center of the compartment), the second compartment was black, covered, and had a grid floor. A guillotine door separated the compartments. On day 9 (training), each animal was placed in the white compartment and was left to explore for 5 s. Then, the door was opened, which allowed the mouse to enter the black compartment. After it had entered, the door was closed, and a foot shock was delivered (0.3 mA) for 3 s generated by a scramble shock generator (Lafayette Instruments, Lafayette, USA). The step-through latency (time the mouse spent in the white compartment after the door was opened) and the level of sensitivity (no sign = 0, flinching reactions = 1, vocalization = 2) were recoded. Treatment with sterubin (1) did not affect the measured parameters. On the next day (day 10), each mouse was placed in the white compartment and was allowed to explore for 5 s. Then, the door was opened allowing the mouse to step over into the black compartment. The step-through latency was measured for up to 300 s.

Sacrifice and brain collection: All animals were sacrificed on day 11. The brains were collected, hippocampus and cortex were isolated, and the samples were frozen at −80 °C.

Statistical analysis: Weight gain and results from the YMT were analyzed by the software GraphPad Prism 5.0 using one-way ANOVA, followed by Dunnett's *post-hoc* multiple comparison test. STPA had a maximum step-through latency of 300 s. Therefore, a Gaussian distribution could not be assumed. The results were analyzed using a Kruskal-Wallis non-parametric ANOVA, followed by a Dunn's multiple comparison test. $p < 0.05$ was considered significant.

Novel-object recognition test: Male C57Bl/6J mice were used and the testing was done by Scripps Research. All mice were acclimated to the colony room for at least 2 weeks prior to testing and were tested at an average age of 8 weeks. Mice were randomly assigned across treatment groups with 11 mice in each group. For each dose tested, a solution of sterubin in corn oil was prepared. The vehicle was corn oil alone. All were administered orally 60 min prior to the training session at a volume of $10\ mL\,kg^{-1}$ body weight. Rolipram was dissolved in 10% DMSO and administered intraperitoneally at $0.1\ mg\,kg^{-1}$ 20 min prior to training. The test was performed as described previously.[29] Briefly, on day 1 mice were habituated to a circular open field arena for one hour in cage groups of four. 24 h later, individual mice were placed back in the same arena which now contained two identical objects for a 15 min training trial. On day 3, vehicle-, sterubin- or rolipram-treated mice were individually placed back in the same arena in the presence of both the familiar object (i.e., previously explored) and a novel object. The spatial positions of the objects were counterbalanced between subjects. Each animal's test trial was recorded and the first 10 min of each session were scored. Object recognition was computed using the formula: Time spent with novel object *x* 100)/Total time spent exploring both objects. Data were analyzed by a one-way ANOVA followed by post-hoc comparisons with Fisher's test.

Conflict of interest

The authors declare no conflict of interest.

[1] a) S. J. Allen, J. J. Watson, D. K. Shoemark, N. U. Barua, N. K. Patel, *Pharmacol. Ther.* **2013**, *138*, 155–175; b) C. Patterson, *Alzheimer's Disease International (ADI)*, London (UK), **2018**.

[2] a) D. J. Selkoe, *Science* **2002**, *298*, 789–791; b) K. Blennow, M. J. de Leon, H. Zetterberg, *Lancet* **2006**, *368*, 387–403.

[3] M. Prior, C. Chiruta, A. Currais, J. Goldberg, J. Ramsey, R. Dargusch, P. A. Maher, D. Schubert, *ACS Chem. Neurosci.* **2014**, *5*, 503–513.

[4] a) P. Agostinho, R. A. Cunha, C. Oliveira, *Curr. Pharm. Des.* **2010**, *16*, 2766–2778; b) C. Hölscher, *EBioMedicine* **2019**, *39*, 17–18.

[5] T. Bui Thanh, H. Nguyen Thanh, *J. Basic. Clin. Physiol. Pharmacol.* **2017**, *28*, 413–423.

[6] a) F. Pohl, P. Kong Thoo Lin, *Molecules* **2018**, *23*, 3283; b) N. Cho, J. H. Choi, H. Yang, E. J. Jeong, K. Y. Lee, Y. C. Kim, S. H. Sung, *Food Chem. Toxicol.* **2012**, *50*, 1940–1945; c) M. Sato, K. Murakami, M. Uno, H. Ikubo, Y. Nakagawa, S. Katayama, K.-i. Akagi, K. Irie, *Biosci. Biotechnol. Biochem.* **2013**, *77*, 1100–1103.

[7] S. Gunesch, S. Schramm, M. Decker, *Future Med. Chem.* **2017**, *9*, 711–713.

[8] S. Schramm, G. Huang, S. Gunesch, F. Lang, J. Roa, P. Högger, R. Sabaté, P. Maher, M. Decker, *Eur. J. Med. Chem.* **2018**, *146*, 93–107.

[9] S. Gunesch, C. Kiermeier, M. Hoffmann, W. Fischer, A. F. M. Pinto, T. Maurice, P. Maher, M. Decker, *Redox Biol.* **2019**, 101378.

[10] S. Schramm, S. Gunesch, F. Lang, M. Saedtler, L. Meinel, P. Högger, M. Decker, *Arch. Pharm. Chem. Life Sci.* **2018**, *351*, 1800206.

[11] W. Fischer, A. Currais, Z. Liang, A. Pinto, P. Maher, *Redox Biol.* **2019**, *21*, 101089.

[12] V. K. Chesnut, *Plants used by the Indians of Mendocino County, California, Vol. 7*, Mendocino County Historical Society, Fort Bragg (CA, USA), **1974**.

[13] a) J. P. Ley, G. Krammer, G. Reinders, I. L. Gatfield, H.-J. Bertram, *J. Agric. Food Chem.* **2005**, *53*, 6061–6066; b) J. Walker, K. V. Reichelt, K. Obst, S. Widder, J. Hans, G. E. Krammer, J. P. Ley, V. Somoza, *Food Func.* **2016**, *7*, 3046–3055.

[14] M. Krause, R. Galensa, *Chromatographia* **1991**, *32*, 69–72.

[15] T. Maurice, B. P. Lockhart, A. Privat, *Brain Res.* **1996**, *706*, 181–193.

[16] H. Wagner, L. Farkas, in *The Flavonoids* (Eds.: J. B. Harborne, T. J. Mabry, H. Mabry), Springer US, Boston, MA, **1975**, 127–213.

[17] E.-M. Jung, Y. R. Lee, *Bull. Korean Chem. Soc.* **2008**, *29*, 1199–1204.

[18] B. Roschek, R. C. Fink, M. D. McMichael, D. Li, R. S. Alberte, *Phytochemistry* **2009**, *70*, 1255–1261.

[19] G. Bringmann, K. Messer, M. Wohlfarth, J. Kraus, K. Dumbuya, M. Rückert, *Anal. Chem.* **1999**, *71*, 2678–2686.

[20] W. Gaffield, *Tetrahedron* **1970**, *26*, 4093–4108.

[21] J. B. Davis, P. Maher, *Brain Res.* **1994**, *652*, 169–173.

[22] a) S. Tan, D. Schubert, P. Maher, *Curr. Top. Med. Chem.* **2001**, *1*, 497–506; b) T. H. Murphy, M. Miyamoto, A. Sastre, R. L. Schnaar, J. T. Coyle, *Neuron*

1989, *2*, 1547 – 1558; c) S. Tan, M. Wood, P. Maher, *J. Neurochem.* **2002**, *71*, 95 – 105.

[23] A. Currais, P. Maher, *Antioxid. Redox Signal.* **2013**, *19*, 813 – 822.

[24] S. A. B. E. Van Acker, D.-j. Van Den Berg, M. N. J. L. Tromp, D. H. Griffioen, W. P. Van Bennekom, W. J. F. Van Der Vijgh, A. Bast, *Free Radical Biol. Med.* **1996**, *20*, 331 – 342.

[25] J. Vrba, R. Gažák, M. Kuzma, B. Papoušková, J. Vacek, M. Weiszenstein, V. Křen, J. Ulrichová, *J. Med. Chem.* **2013**, *56*, 856 – 866.

[26] H. Aft, *J. Org. Chem.* **1965**, *30*, 897 – 901.

[27] V. Lahmy, J. Meunier, S. Malmström, G. Naert, L. Givalois, S. H. Kim, V. Villard, A. Vamvakides, T. Maurice, *Neuropsychopharmacology* **2013**, *38*, 1706 – 1723.

[28] a) P. Lu, T. Mamiya, L. Lu, A. Mouri, L. Zou, T. Nagai, M. Hiramatsu, T. Ikejima, T. Nabeshima, *Br. J. Pharmacol.* **2009**, *157*, 1270 – 1277; b) S. Saito, Y. Yamamoto, T. Maki, Y. Hattori, H. Ito, K. Mizuno, M. Harada-Shiba, R. N. Kalaria, M. Fukushima, R. Takahashi, M. Ihara, *Acta Neuropathol. Commun.* **2017**, *5*, 26.

[29] P. Maher, T. Akaishi, K. Abe, *Proc. Natl. Acad. Sci. USA* **2006**, *103*, 16568 – 16573.

[30] R. Bourtchouladze, R. Lidge, R. Catapano, J. Stanley, S. Gossweiler, D. Romashko, R. Scott, T. Tully, *Proc. Natl. Acad. Sci. USA* **2003**, *100*, 10518 – 10522.

[31] H. Takahashi, S. Li, Y. Harigaya, M. Onda, *Heterocycles* **1987**, *26*, 3239 – 3248.

[32] a) T. Bruhn, A. Schaumlöffel, Y. Hemberger, G. Bringmann, *Chirality* **2013**, *25*, 243 – 249; b) T. Bruhn, A. Schaumlöffel, Y. Hemberger, G. Pescitelli, **2017**, SpecDis, Version 1.71; www.specdis-software.jimdo.com.

[33] a) M. Scheiner, D. Dolles, S. Gunesch, M. Hoffmann, M. Nabissi, O. Marinelli, M. Naldi, M. Bartolini, S. Petralla, E. Poeta, B. Monti, C. Falkeis, M. Vieth, H. Hübner, P. Gmeiner, R. Maitra, T. Maurice, M. Decker, *J. Med. Chem.* **2019**, *62*, 9078 – 9102; b) M. Hoffmann, C. Stiller, E. Endres, M. Scheiner, S. Gunesch, C. Sotriffer, T. Maurice, M. Decker, *J. Med. Chem.* **2019**, *62*, 9116 – 9140; c) T. Maurice, M. Strehaiano, N. Siméon, C. Bertrand, A. Chatonnet, *Behav. Brain Res.* **2016**, *296*, 351 – 360.